Totally asymmetric simple exclusion process with a shortcut

2007 J. Phys. A: Math. Theor. 40 12351

(http://iopscience.iop.org/1751-8121/40/41/006)

IOP Publishing Journal of Physics A: Mathematical and Theoretical

J. Phys. A: Math. Theor. **40** (2007) 12351–12364 doi:10.1088/1751-8113/40/41/006

Totally asymmetric simple exclusion process with a shortcut

Yao-Ming Yuan[1], Rui Jiang[1], Ruili Wang[2], Mao-Bin Hu[1] and Qing-Song Wu[1]

[1] School of Engineering Science, University of Science and Technology of China, Hefei, Anhui, 230026, People's Republic of China
[2] Institute of Information Sciences and Technology, Massey University, New Zealand

Received 27 February 2007, in final form 29 August 2007
Published 25 September 2007
Online at stacks.iop.org/JPhysA/40/12351

Abstract

In this paper, we study the interplay of a totally asymmetric simple exclusion process (TASEP) with a shortcut in its bulk under open boundary conditions. Two different models are introduced: (i) model A for molecular motor motion, and (ii) model B for vehicular traffic. The phase diagrams and density profiles of both models are studied. It is found that although the phase diagrams of both models can be classified into three regions, the phases corresponding to these regions and the phase boundaries between these regions are quite different in these two models. Moreover, the approximate stationary-state solutions of model A have been carried out and it is shown that the analytical results are in good agreement with the results of Monte Carlo simulations.

PACS numbers: 05.70.Ln, 02.50.Ey, 05.60.Cd

(Some figures in this article are in colour only in the electronic version)

1. Introduction

One-dimensional asymmetric simple exclusion processes (ASEPs), which represent one of the basic models in studying the rich behavior of complex systems held far from equilibrium, have been intensively studied for decades (see reviews in [1, 2]). ASEP was first introduced in [3] for ribosome motion and then used to model a wide variety of physical processes including surface growth [4, 5], traffic flow [6], etc.

ASEPs are discrete non-equilibrium models that describe the stochastic dynamics of multi-particle transport along one-dimensional lattices. Each lattice site can be either empty or occupied by a single particle. Particles interact only through hard core exclusion potential. The simplest limit of an ASEP is that particles can only move in one direction. This is called the totally asymmetric simple exclusion processes (TASEP). Exact analytical solutions for stationary states exist under periodic [7, 8] and open boundary conditions [9, 10] and

different update schemes [11–13]. These studies contribute to better understanding of general mechanisms leading to phase transitions in the systems that are out of equilibrium.

Under open boundary conditions, the solutions yield phase diagrams with three phases [9, 10]. At small values of injection rates $\alpha < 0.5$ and $\alpha < \beta$, the system is found in a low-density entry-limited phase where

$$\begin{aligned} &\rho_1 = \alpha \qquad \rho_L = \frac{\alpha(1-\alpha)}{\beta} \\ &J = \alpha(1-\alpha) \qquad \rho_{\text{bulk}} = \alpha, \end{aligned} \tag{1}$$

where ρ_1, ρ_L and ρ_{bulk} are the densities at the entrance, exit and the bulk of the lattice far away from the boundaries, respectively. J denotes the flux.

At small values of extraction rates $\beta < 0.5$ and $\beta < \alpha$, the system is in a high-density exit-limited phase with

$$\begin{aligned} &\rho_1 = 1 - \frac{\beta(1-\beta)}{\alpha} \qquad \rho_L = 1-\beta \\ &J = \beta(1-\beta) \qquad \rho_{\text{bulk}} = 1-\beta. \end{aligned} \tag{2}$$

Moreover, at large values of the injection ($\alpha \geqslant 0.5$) and extraction ($\beta \geqslant 0.5$) rates the system is in a maximal current phase with

$$\begin{aligned} &\rho_1 = 1 - \frac{1}{4\alpha} \qquad \rho_L = \frac{1}{4\beta} \\ &J = \frac{1}{4} \qquad \rho_{\text{bulk}} = \frac{1}{2}. \end{aligned} \tag{3}$$

A number of different extensions of ASEPs have been proposed, including particles occupying more than one lattice site [14, 15], defects in the bulk [16–20], particle moving in system with periodically varying sitewise disorder [21], combination of random particles attachment and detachment [22], two-lane extensions [23–28], allowance of long-range hopping [29], and so on.

In 2004, Brankov *et al* [30] and Pronina and Kolomeisky [31] in 2005 investigated a problem of ASEP with double-chain section in the middle, where they assumed that the particles choose one of the two chains with an equal probability 0.5 and that the lengths of the two chains equal to each other. However, asymmetric conditions that the particles choose two chains with different probabilities and the lengths of the two chains differ from each other have not been considered yet.

In this paper, we investigated an extension of a TASEP, in which a shortcut is presented in the bulk, i.e. the length of one chain (shortcut) is zero. The study may be relevant for both molecular motor motion and vehicular traffic, because the filament on which the motor moves may be twisted as shown in figure 1(*a*) so that a motor may have a chance to jump directly from k_1 to k_2 with probability q. In vehicular traffic, some drivers may know some shortcuts between two locations while others do not.

Based on these assumptions, we study two different models in this paper. Model A simulates the behavior of molecular motor motion in the presence of a shortcut, while model B simulates the vehicular traffic with a shortcut. The phase diagram and density profiles of both models are analyzed in detail.

The paper is organized as follows. Section 2 introduces the rules of these two models. Simulation and analytic results are presented in section 3. Finally, conclusion is given in section 4.

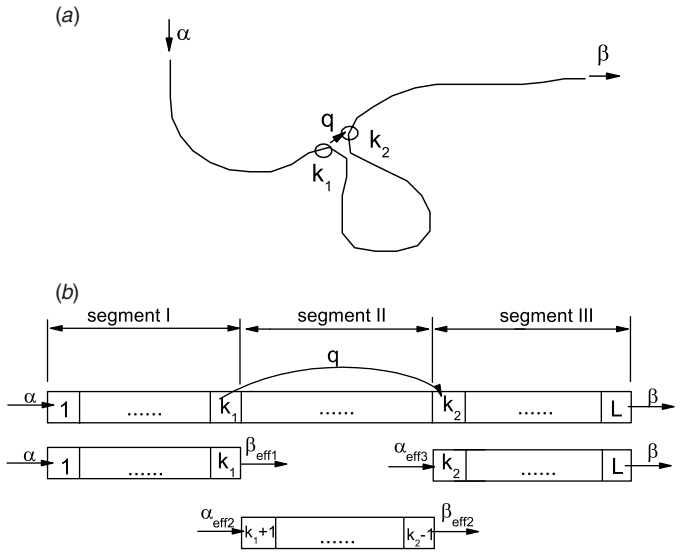

Figure 1. (*a*) The filament of molecular motor motion or lane of vehicular traffic including a shortcut. (*b*) One-dimensional lattice with a shortcut in its bulk abstracted from (*a*).

2. Rules of two models

In this section, the rules of these two different models are introduced. The sketch of lattices is shown in figure 1(*b*). One can see that the lattices are divided into three segments by sites k_1 and k_2. Segments I, II, III start from sites 1, $k_1 + 1, k_2$ and end in sites $k_1, k_2 - 1, L$, respectively.

In model A, all the particles traveling in the lattices are identical to each other. The random update rules are adopted. A site i ($1 \leqslant i \leqslant L$) is chosen randomly. In an infinitesimal time interval $\mathrm{d}t$, if $i = 1$, a particle is inserted with probability $\alpha\,\mathrm{d}t$, provided the site is empty. If site 1 is occupied, the particle moves into site 2 with probability $\mathrm{d}t$ provided site 2 is empty. If $i = L$ and site L is not empty, the particle will leave the system with probability $\beta\,\mathrm{d}t$. If $1 < i < k_1$ or $k_1 < i < L$ and site i is occupied, the particle in site i will move into site $i + 1$ with probability $\mathrm{d}t$ provided site $i + 1$ is empty. However, if $i = k_1$ and site k_1 is occupied by a particle, we have the following:

- If both sites $k_1 + 1$ and k_2 are empty, then the particle in site k_1 moves into site k_2 with probability $q\,\mathrm{d}t$ and moves into site $k_1 + 1$ with probability $(1 - q)\,\mathrm{d}t$.
- If site k_2 is empty and site $k_1 + 1$ is occupied, then the particle in site k_1 moves into site k_2 with probability $q\,\mathrm{d}t$.
- If site k_2 is occupied and site $k_1 + 1$ is empty, then the particle in site k_1 moves into site $k_1 + 1$ with probability $\mathrm{d}t$.
- If both sites $k_1 + 1$ and k_2 are occupied, then the particle does not move.

Note model A reduces to an original TASEP model in the limit $q = 0$.

Different from model A, there are two types of particles in model B. Some particles, denoted by type 1, are aware of the existence of the shortcut and the others, denoted by type 2, do not know this shortcut or do not want to use the shortcut. The random-updating rules of model B differ from that of model A only on sites 1 and k_1.

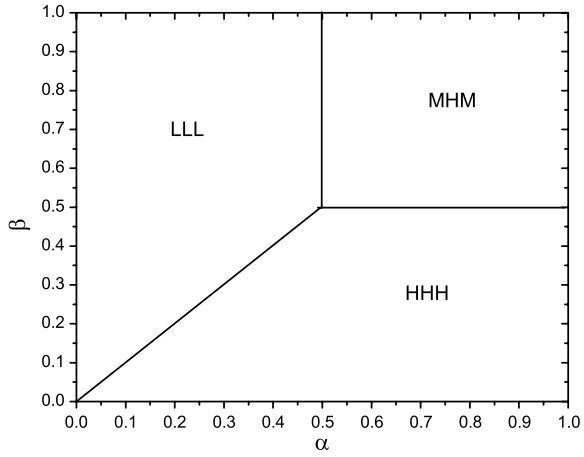

Figure 2. Phase diagram of model A related to α and β.

In an infinitesimal time interval dt, for site 1, if it is empty, a particle is inserted with probability $\alpha\,\mathrm{d}t$. The inserted particle is of type 1 with probability q and of type 2 with probability $1-q$. For site k_1, if it is occupied by a particle of type 1, the particle will move into site k_2 through the shortcut with probability dt provided site k_2 is empty; otherwise the particle will stop at site k_1 until site k_2 is empty; if site k_1 is occupied by a particle of type 2, the particle will move forward into site k_1+1 with probability dt provided site k_1+1 is empty, otherwise the particle will stop at site k_1 until site k_1+1 is empty. Particles of type 1 will always use the shortcut and particles of type 2 never pass through the shortcut. Note that when $q=0$, the system reduces to the original TASEP with system length L; When $q=1$, the system reduces to the original TASEP with system length $\frac{2}{3}L$ and segment II is excluded from the system.

3. Results of model A

In the simulations, the system size is set to $L=3000$ unless otherwise mentioned. We set $k_1=L/3$ and $k_2=2L/3+1$. In other words, the shortcut starts from site $L/3+1$ and ends at site $2L/3$.

In this section, we carry out the simulations of model A. A phase diagram related to α and β is shown in figure 2. Similar to the phase diagram of an original TASEP [9, 10], the phase diagram of model A can be classified into three regions. When $\alpha<0.5$ and $\alpha<\beta$, the three segments of the system are all in the low-density phase (LLL), as shown in figure 3(*a*), where we see the density profiles with the parameters $\alpha=0.3$, $\beta=0.8$ and $q=0.1, 0.3, 0.5, 0.7$ and 0.9. The bulk densities of segments I and III are equal and both equal to α. The shortcut only affects the density of segment II, which is lower than α because some particles pass through the shortcut directly. Consequently, with increase of q, the density of segment II decreases.

When $\beta<0.5$ and $\alpha>\beta$, all three segments of the system are in the high-density phase (HHH). The density profiles with parameters $\alpha=0.8$, $\beta=0.3$ and $q=0.1, 0.3, 0.5, 0.7$ and 0.9 are shown in figure 3(*b*). The densities of segments I and III both equal to $1-\beta$ and

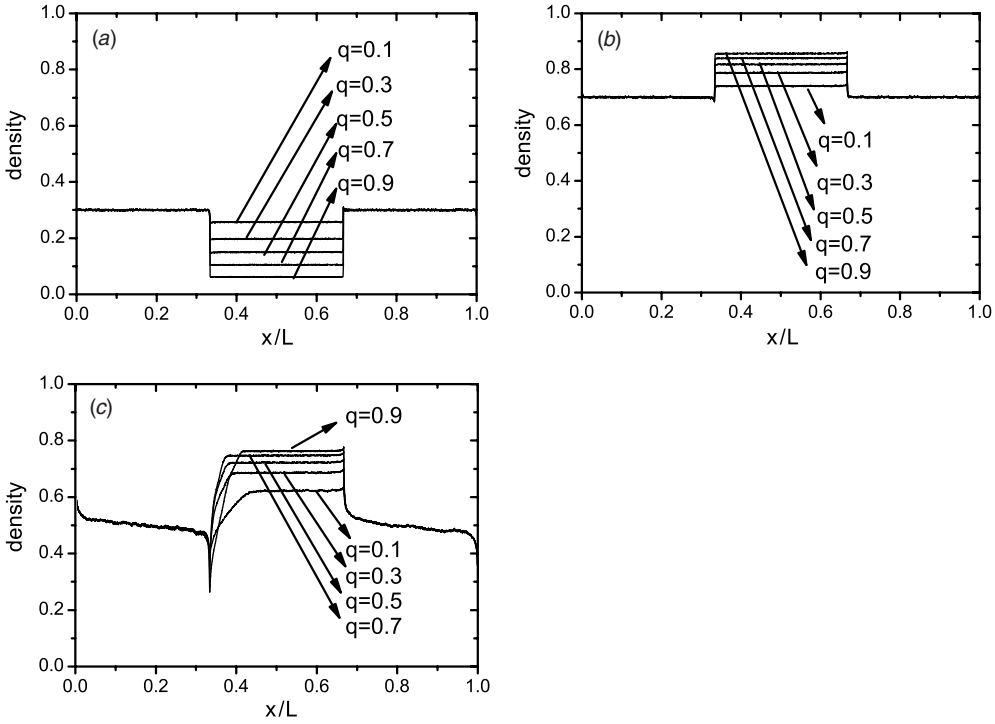

Figure 3. Density profiles of the simulation results of model A corresponding to different phases with $q = 0.1, 0.3, 0.5, 0.7$ and 0.9. (a) $\alpha = 0.3$ and $\beta = 0.8$; (b) $\alpha = 0.8$ and $\beta = 0.3$; (c) $\alpha = 0.8$ and $\beta = 0.8$.

the density of segment II is larger than $1 - \beta$. The density of segment II increases with the increase of q.

When $\alpha \geqslant 0.5$ and $\beta \geqslant 0.5$, segment I, II and III are in the maximal current phase, high-density phase and maximal current phase (MHM), respectively. Figure 3(c) shows the density profiles with parameters $\alpha = 0.8$, $\beta = 0.8$ and $q = 0.1, 0.3, 0.5, 0.7$ and 0.9.

Different from the second-order phase transition between the low-density phase and maximum flow phase in the original phase diagram of a TASEP, the transition between the LLL and MHM phases in model A is of first order if we take the bulk density in segment II as an order parameter. The phase transition between the HHH and MHM phases is of second order, which are the same as the situations in the original TASEP phase diagram.

3.1. Mean field analysis

In this subsection, we present the approximate stationary solutions of model A by using the mean field method proposed in [19]. As illustrated in figure 1(b), three segments are divided and each segment can be regarded as a lattice of a separated TASEP. Moreover, the injection rate and extraction rate of segment I are denoted by α_{eff1} and β_{eff1}, α_{eff2} and β_{eff2} for segment II and α_{eff3} and β_{eff3} for segment III, respectively. Their values are as follows:

$$\begin{aligned} &\alpha_{\text{eff1}} = \alpha \qquad \beta_{\text{eff1}} = 1 - \rho_{k_1+1} + q \cdot \rho_{k_1+1} \cdot \left(1 - \rho_{k_2}\right) \\ &\alpha_{\text{eff2}} = \rho_{k_1}\left[1 - q\left(1 - \rho_{k_2}\right)\right] \qquad \beta_{\text{eff2}} = 1 - \rho_{k_2} \end{aligned} \tag{4}$$

$$\alpha_{\text{eff3}} = q\rho_{k_1} + \rho_{k_2-1} \qquad \beta_{\text{eff3}} = \beta,$$
$$J_{sc} = q\rho_{k_1}(1-\rho_{k_2})$$

where ρ_i represents the stationary value of the density of site i ($i = 1, 2, \ldots, L$). We denote the flux of segments I, II and III, and shortcut as J_1, J_2, J_3 and J_{sc} respectively. Due to particle conservation of the system, we have

$$J_1 = J_2 + J_{sc} = J_3. \tag{5}$$

Next we demonstrate that segments I and III should be in the same phase if $\alpha \neq \beta$. Due to particle conservation, it is impossible that one of them is in maximum-current phase but the other is not. Therefore, we only need to demonstrate that the following four possibilities do not exist: (L, L, H), (L, H, H), (H, L, L) and (H, H, L). Here (X, Y, Z) denotes that segment I, II and III is in the X phase, Y phase and Z phase, respectively.

Suppose the system is in (L, L, H) or (L, H, H), this implies $\alpha < 0.5$, $J_1 = \alpha(1-\alpha)$, $\beta < 0.5$ and $J_3 = \beta(1-\beta)$. Together with equation (5) and $\alpha \neq \beta$, we obtain $\alpha + \beta = 1$, which is contradicted with $\alpha < 0.5$ and $\beta < 0.5$. Thus, the phase (L, L, H) or (L, H, H) cannot exist.

Suppose the system is in (H, L, L), then we have $1 - \rho_{k_1} = \rho_{k_2}$ due to $J_1 = J_3$. From equation (5), we obtain $\rho_{k_1}(1-\rho_{k_1}) = \alpha_{\text{eff2}}(1-\alpha_{\text{eff2}}) + q\rho_{k_1}(1-\rho_{k_2})$, from which we can obtain $\rho_{k_1} = 0$. Thus, the system cannot be in (H, L, L).

If the system is in (H, H, L), then $J_2 = \beta_{\text{eff2}}(1-\beta_{\text{eff2}}) = \rho_{k_2}(1-\rho_{k_2}) = J_3$, which is contradicted with $J_3 > J_2$ when $q \neq 0$. Thus, the system cannot be in (H, H, L) either.

Therefore, the same as the original TASEP, three different situations for segments I and III can be classified.

When $\alpha < 0.5$ and $\alpha < \beta$, both segments I and III are in the low-density phase. Therefore,

$$\begin{aligned} J_2 &= \alpha_{\text{eff2}}(1-\rho_{k_1+1}) = \rho_{k_2-1}\beta_{\text{eff2}} \\ J_1 &= J_3 = \alpha(1-\alpha) \\ \alpha_{\text{eff3}} &= \rho_{k_2} = \alpha. \end{aligned} \tag{6}$$

If we assume that segment II is in the high-density phase, then $\rho_{k_2-1} = 1 - \beta_{\text{eff2}} = \rho_{k_2}$. From equation (6), we obtain $J_2 = \alpha(1-\alpha) = J_1 = J_3$, which is unreasonable when $q \neq 0$. Thus, segment II cannot be in the high-density phase. It is easy to understand that segment II cannot be in the maximal current phase. Therefore, segment II can only be in the low-density phase. Thus,

$$\rho_{k_1+1} = \alpha_{\text{eff1}}. \tag{7}$$

From equations (1), (4)–(7), we can obtain approximate solutions under the conditions of $\alpha < 0.5$ and $\alpha < \beta$:

$$\begin{aligned} \rho_{k_1} &= \frac{1 - \sqrt{1 - 4\alpha(1-\alpha)[1-q(1-\alpha)]^2}}{2[1-q(1-\alpha)]^2} \\ \rho_{k_1+1} &= \alpha_{\text{eff2}} = \rho_{k_1}(1-q+q\alpha) \\ \beta_{\text{eff1}} &= \frac{\alpha(1-\alpha)}{\rho_{k_1}} \\ \beta_{\text{eff2}} &= 1-\alpha \\ \alpha_{\text{eff3}} &= q(1-\alpha)\rho_{k_1}. \end{aligned} \tag{8}$$

When $\beta < 0.5$ and $\alpha > \beta$, segments I and III are both corresponding to the high-density phase. Then, we can obtain $\rho_{k_1} = 1 - \beta$. From flux conversation, we can obtain that

$$(q\rho_{k_1} + \rho_{k_2-1})(1-\rho_{k_2}) = \beta(1-\beta) \tag{9}$$

thus,

$$\rho_{k_2-1} = \frac{\beta(1-\beta)}{1-\rho_{k_2}} - q(1-\beta). \tag{10}$$

Similarly, segment II cannot be in the maximal-flow phase because we can obtain $J_{sc} < 0$ from $J_1 = J_2 + J_{sc}$. If we assume that segment II is in the low-density phase, according to equations (1) and (4), we can obtain the mean density of the exiting site of segment II,

$$\begin{aligned}\rho_{k_2-1} &= \frac{\alpha_{\text{eff2}}(1-\alpha_{\text{eff2}})}{\beta_{\text{eff2}}} \\ &= \frac{(1-\beta)\big[\rho_{k_2} + \big(1-\rho_{k_2}\big)(1-q)\big]\big\{1-(1-\beta)\big[\rho_{k_2} + \big(1-\rho_{k_2}\big)(1-q)\big]\big\}}{1-\rho_{k_2}}.\end{aligned} \tag{11}$$

From equations (10) and (11), we can obtain the equation

$$\big(1+q+q\rho_{k_2}\big)^2 = 1, \tag{12}$$

which has no solutions when $q > 0$ and $\rho_{k_2} > 0$. Therefore, segment II cannot be in the low-density phase.

Segment II can only be in the high-density phase. Then, $\rho_{k_2-1} = 1 - \beta_{\text{eff2}} = \rho_{k_2}$. From equation (9), we can obtain

$$\rho_{k_2}^2 - [1-q(1-\beta)]\rho_{k_2} + (\beta-q)(1-\beta) = 0, \tag{13}$$

thus

$$\begin{aligned}\rho_{k_2} &= \frac{1-q(1-\beta)+\sqrt{[1-q(1-\beta)]^2 - 4(\beta-q)(1-\beta)}}{2} \\ \beta_{\text{eff1}} &= \beta \\ \alpha_{\text{eff2}} &= \rho_{k_1}\big[1-q\big(1-\rho_{k_2}\big)\big] = (1-\beta)\big[1-q\big(1-\rho_{k_2}\big)\big] \\ \beta_{\text{eff2}} &= 1-\rho_{k_2} = \frac{1+q(1-\beta)-\sqrt{[1-q(1-\beta)]^2 - 4(\beta-q)(1-\beta)}}{2} \\ \alpha_{\text{eff3}} &= \rho_{k_2} = \frac{1-q(1-\beta)+\sqrt{[1-q(1-\beta)]^2 - 4(\beta-q)(1-\beta)}}{2}.\end{aligned} \tag{14}$$

When $\alpha \geqslant 0.5$ and $\beta \geqslant 0.5$, segments I and III are in the maximal current phase. It is clear that segment II cannot be in the maximal current phase due to $J_{sc} > 0$. If we assume that segment II is in the low-density phase, then the bulk density in segment II is ρ_{k_1+1} and we have

$$\rho_{k_1+1}\big(1-\rho_{k_1+1}\big) = \rho_{k_2-1}\big(1-\rho_{k_2}\big). \tag{15}$$

On the other hand, the density profile in segment II has an increasing tail near the right end due to high density at site k_2. Therefore, we believe that the density on site $k_2 - 1$ is approximately the same as that on site k_2, i.e.,

$$\rho_{k_2-1} \approx \rho_{k_2}. \tag{16}$$

It is obvious that the sum of the flow rate of segment II and that of the shortcut is 0.25, i.e.,

$$q\rho_{k_1}\big(1-\rho_{k_2}\big) + q\rho_{k_1}\rho_{k_2}\big(1-\rho_{k_1+1}\big) + (1-q)\rho_{k_1}\big(1-\rho_{k_1+1}\big) = 0.25. \tag{17}$$

Finally, we have

$$q\rho_{k_1}\rho_{k_2}\big(1-\rho_{k_1+1}\big) + (1-q)\rho_{k_1}\big(1-\rho_{k_1+1}\big) = \rho_{k_2-1}\big(1-\rho_{k_2}\big). \tag{18}$$

It is difficult to express the solutions of equations (15)–(18) analytically. Nevertheless, it is found numerically that reasonable solutions do not exist. Therefore, segment II cannot be in the low-density phase.

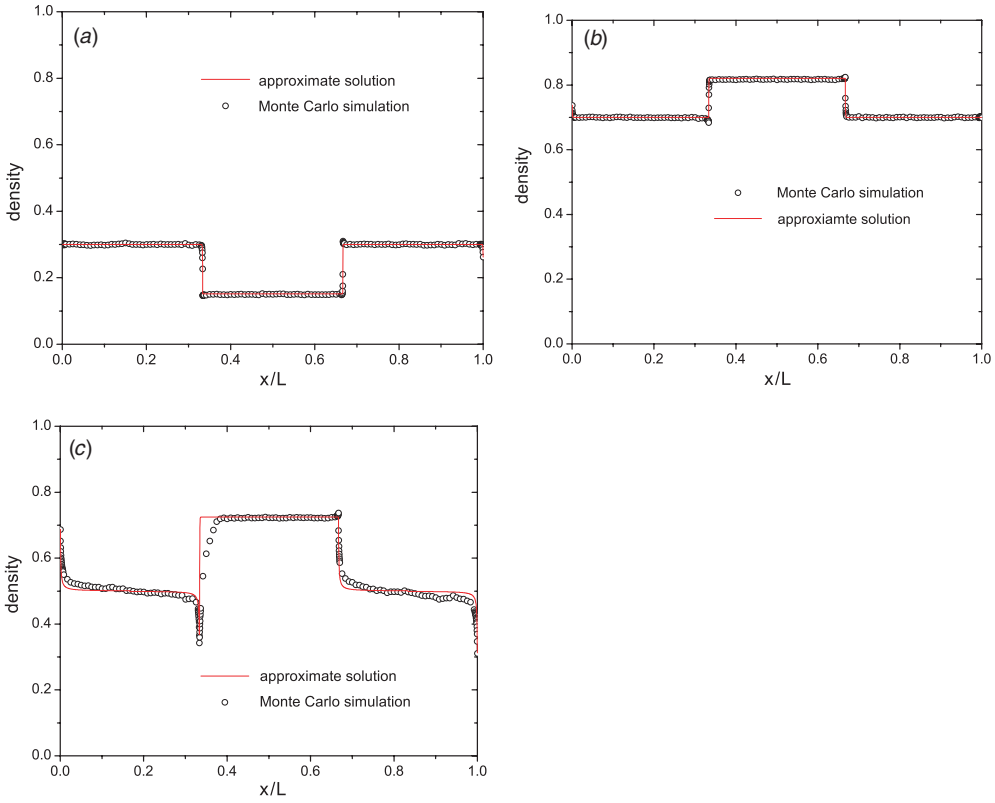

Figure 4. Comparison of approximate solutions and Monte Carlo simulation results for model A corresponding to different phases. (*a*) $\alpha = 0.3$, $\beta = 0.8$ and $q = 0.5$; (*b*) $\alpha = 0.8$, $\beta = 0.3$ and $q = 0.5$; (*c*) $\alpha = 0.8$, $\beta = 0.8$ and $q = 0.5$.

When segment II is in the high-density phase, the bulk density in segment II is ρ_{k_2-1} and we have

$$\rho_{k_2-1}\left(1-\rho_{k_2-1}\right) = \rho_{k_2-1}\left(1-\rho_{k_2}\right). \tag{19}$$

The density profile in segment II has an decreasing tail near the left end due to small density at site k_1. Similarly, we believe that the density on site $k_1 + 1$ is approximately the same as that on site k_1 (which is also supported by numerical simulations), i.e.,

$$\rho_{k_1} \approx \rho_{k_1+1}. \tag{20}$$

It is also difficult to express the solutions of equations (17)–(20) analytically, but the numerical solutions can be obtained.

The density profiles of Monte Carlo simulations and our approximate solutions have been compared in figure 4. It is shown that our approximate solutions are in good agreement with the Monte Carlo simulation results.

3.2. Phase boundary

This subsection focuses on the phase boundary between LLL and HHH in model A. Figure 5 shows the density profiles at the phase boundary with parameters $\alpha = \beta = 0.25$, $q =$

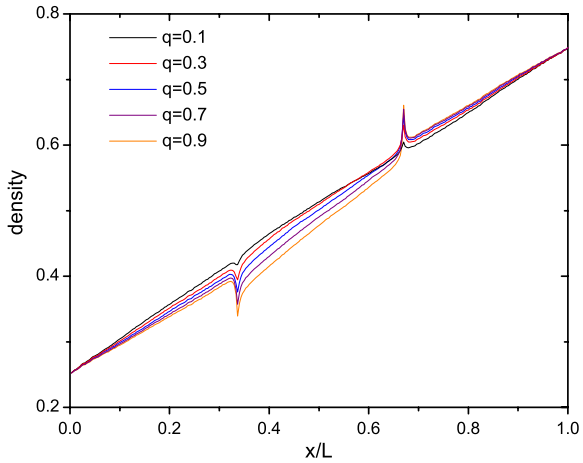

Figure 5. Density profiles of the simulation results of model A at the phase boundary with parameters $L = 300$, $\alpha = \beta = 0.25$, $q = 0.1, 0.3, 0.5, 0.7$ and 0.9.

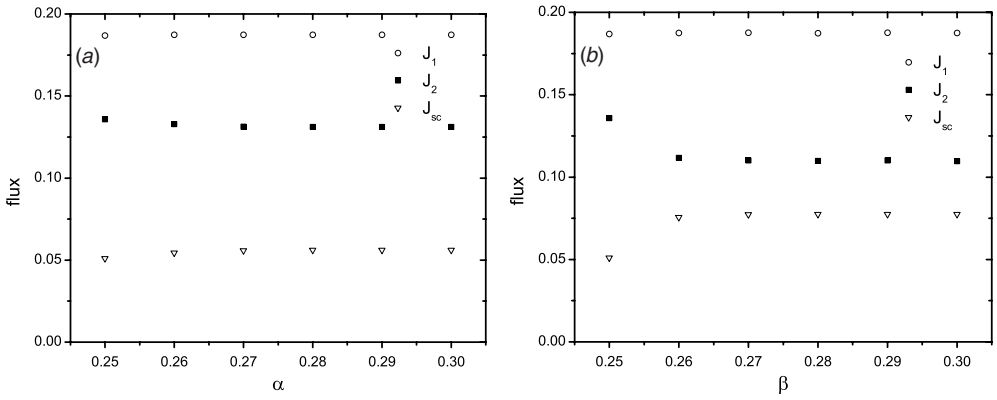

Figure 6. Fluxes of segment I and II and shortcut of model A near the phase boundary with parameters $\alpha = \beta = 0.25$, $q = 0.5$. (a) versus α with $\beta = 0.25$; (b) versus β with $\alpha = 0.25$.

0.1, 0.3, 0.5, 0.7 and 0.9. It is found that the slopes of segment I and III approximately equal to each other and they increase with the decrease of q. In contrast, the slope of segment II decreases with the increase of q.

Figures 6(a) and (b) show J_1, J_2 and J_{sc} versus α with β fixed and versus β with α fixed, respectively. As expected, J_1 is continuous when crossing the phase boundary $\alpha = \beta$. However, it is interesting to find out J_2 is discontinuous when crossing the phase boundary. This is also supported by mean field approximation (see equations (2), (8) and (14)). The result is qualitatively different from the results in [30], in which the flux on the middle chains is continuous when crossing the corresponding phase boundary. Furthermore, it is found that J_2 corresponding to $\alpha = \beta$ approximately equals to that corresponding to $\alpha > \beta$, provided β does not change. This result is obviously related to the asymmetric hopping of particles at site k_1, although presently we do not know the exact reason, which needs to be further investigated in future work.

Given this fact, J_2 corresponding to $\alpha = \beta$ could be calculated by equations (2) and (14). As a result, the density profile corresponding to $\alpha = \beta$ could be calculated by the domain wall approach proposed in [31] as follows.

A position of the domain wall in the system is denoted by x: $x = \frac{i}{L}$ where i is the site index and L is the length of the system. Therefore, the cases of $0 < x \leqslant 1/3$, $1/3 < x \leqslant 2/3$ and $2/3 < x \leqslant 1$ describe segments I, II and III, respectively. The moving rate of the domain wall in segments I, II and III are u_1, u_2 and u_3, which can be determined by utilizing the expression below:

$$u_k = \frac{J_k}{\rho_+^k - \rho_-^k}, \qquad \text{for} \quad k = 1, 2, 3, \tag{21}$$

where

$$\begin{aligned} &\rho_-^1 = \alpha, \qquad \rho_+^1 = 1 - \alpha, \\ &\rho_-^2 = \frac{1 - \sqrt{1 - 4J_2}}{2}, \qquad \rho_+^2 = \frac{1 + \sqrt{1 - 4J_2}}{2}, \\ &\rho_-^3 = \beta, \qquad \rho_+^3 = 1 - \beta. \end{aligned} \tag{22}$$

We introduce three probabilities P_1, P_2 and P_3 of finding the domain wall at any position in segments I, II and III. These probabilities are obviously normalized:

$$P_1 + P_2 + P_3 = 1. \tag{23}$$

Then, at the two junctions we have

$$\frac{u_1 P_1}{L/3}\frac{J_2}{J_1} = \frac{u_2 P_2}{L/3} = \frac{u_3 P_3}{L/3}\frac{J_2}{J_1}. \tag{24}$$

By combining the last two equations we can solve the value of P_1, P_2 and P_3. Then we can determine the probabilities of the domain wall at any position less than a certain value of x:

$$\begin{aligned} &\text{Prob}(x_{DW} < x) = \frac{P_1 x}{1/3}, \qquad 0 < x \leqslant 1/3 \\ &\text{Prob}(x_{DW} < x) = P_1 + \frac{P_2(x - 1/3)}{1/3}, \qquad 1/3 < x \leqslant 2/3 \\ &\text{Prob}(x_{DW} < x) = P_1 + P_2 + \frac{P_3(x - 2/3)}{1/3}, \qquad 2/3 < x \leqslant 1. \end{aligned} \tag{25}$$

Finally, the density at any position can be calculated as

$$\rho(x) = \rho_-^k \,\text{Prob}(x_{DW} > x) + \rho_+^k \,\text{Prob}(x_{DW} < x). \tag{26}$$

Substituting the value of $\alpha = 0.25, \beta = 0.25, q = 0.5 J_1 = 0.1875$ and $J_2 = 0.13$ into the equations above, we can obtain the analytic results of density profiles at the phase boundary $\alpha = \beta = 0.25$:

$$\begin{aligned} &\rho(x) = 0.25 + 0.4425x, \qquad 0 < x \leqslant 1/3 \\ &\rho(x) = 0.85x + 0.0745, \qquad 1/3 < x \leqslant 2/3 \\ &\rho(x) = 0.4425x + 0.3075, \qquad 2/3 < x \leqslant 1. \end{aligned} \tag{27}$$

Figure 7 shows the comparison of simulation results and the analytic results. It is shown that the simulation results are in good agreement with analytic results in segments I and III and they only slightly deviate from the analytic results in segment II.

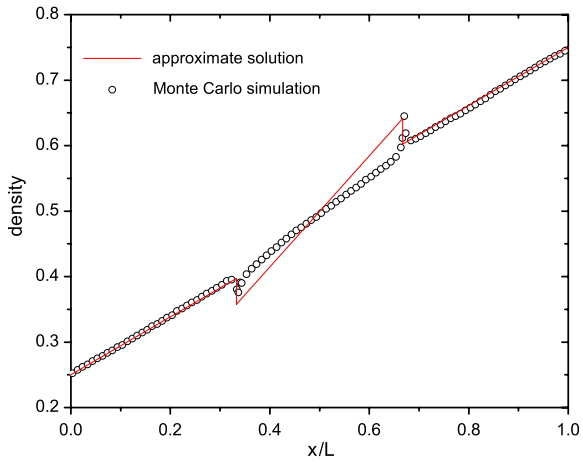

Figure 7. Comparison of results of the domain wall approach and that of simulation at the phase boundary $\alpha = \beta = 0.25$ and $q = 0.5$.

The slope of segment I increases with the decrease of q can also be explained with the approach. From equations (21)–(26), we can obtain the slope of segments I and II, denoted by s_1 and s_2:

$$s_1 = \frac{3}{2 + 2\sqrt{1 - 4J_2}} \qquad s_2 = \frac{3(1 - 4J_2)}{1 + \sqrt{1 - 4J_2}}. \tag{28}$$

When q decreases, J_2 increases. As a result, s_1 increases and s_2 decreases corresponding to the parameters used.

4. Results of model B

The simulations of model B are described in this section. The phase diagram of model B is shown in figure 8. One can see that three regions can be classified. Region I corresponds to the LLL phase: all three segments are in the low-density phase. The corresponding density profiles with $\alpha = 0.3, \beta = 0.8$ and different values of q are illustrated in figure 9(a). We can see that the bulk densities of both segments I and III are equal to α and the bulk density of segment II decreases with the increase of q. Moreover, comparing with the case in model A, the bulk density of segment II in model B is smaller under the same parameters set. It is because the particles of type 1 do not enter segment II at all in model B.

Region II corresponds to the MLM phase of the system where segments I, II and III correspond to the maximal current phase, low-density phase, maximal current phase, respectively. The corresponding density profiles are shown in figure 9(b). Comparing with the case in model A, the maximal current phases in segments I and III are different. Instead of 0.5, the bulk densities of segments I and III are $1 - \lambda$ and λ respectively and the maximal current equals to $\lambda(1 - \lambda)$ instead of $\frac{1}{4}$. Here, $\lambda < 0.5$ is a parameter dependent of q and it decreases with the increase of q. In particular, segment II is in a low-density phase, which is different from the case in model A where segment II is in the high-density phase.

The phase in region III depends on q. When q is larger than a threshold $q_c \approx 0.27$, region III corresponds to the HLH phase: segments I and III are in the high-density phase but segment II is in the low-density phase. See, for example, the density profiles corresponding

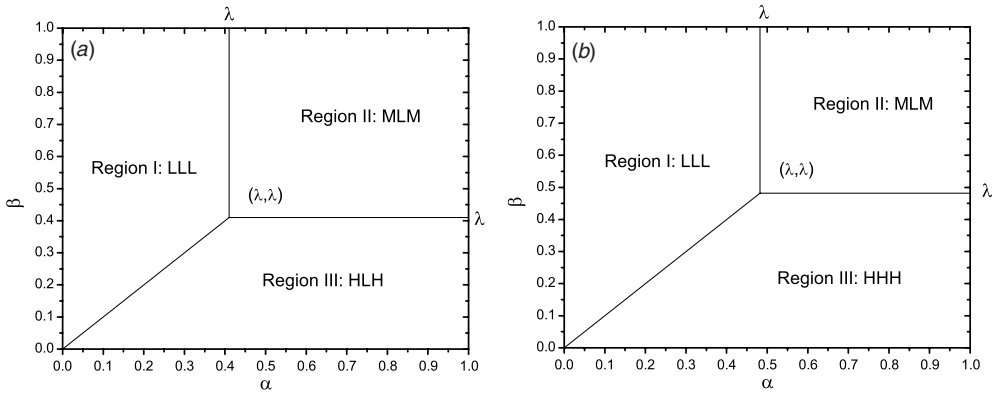

Figure 8. Phase diagrams of model B related to α and β. (*a*) $q = 0.5 > q_c$; (*b*) $q = 0.1 < q_c$.

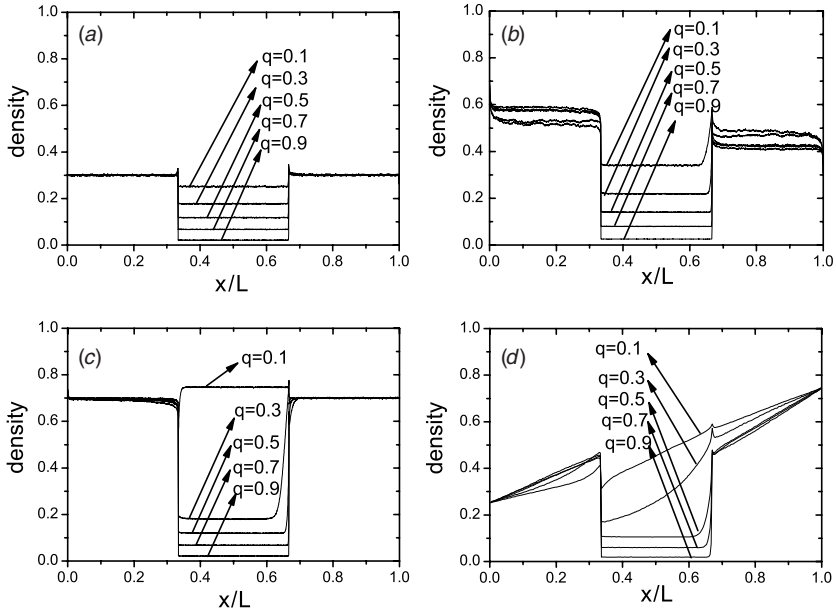

Figure 9. Density profiles of simulation results for model B corresponding to different phases with $q = 0.1, 0.3, 0.5, 0.7$ and 0.9. (*a*) $\alpha = 0.3$ and $\beta = 0.8$; (*b*) $\alpha = 0.8$ and $\beta = 0.8$; (*c*) $\alpha = 0.8$ and $\beta = 0.3$; (*d*) $\alpha = 0.25$ and $\beta = 0.25$.

to $q = 0.3, 0.5, 0.7$ and 0.9 in figure 9(*c*). When $q < q_c$, region III corresponds to the HHH phase: all three segments are in the high-density phase. See, for example, the density profiles corresponding to $q = 0.1$ in figure 9(*c*).

We would like to point out all the boundaries in the phase diagram corresponding to a first-order transition. From the LLL phase to the MLM phase, the bulk density in segment I is discontinuous. From the LLL phase to the HLH phase, there is a jump of bulk densities in segments I and III. From the MLM phase to the HHH phase, a jump of bulk densities

in segments II and III occurs. From the MLM phase to the HLH phase, the bulk density is discontinuous in segment III.

Finally we discuss the phase boundary $\alpha = \beta$. The simulations show that the density profile in segments I and III is always linear. The density profile in segment II is linear if $q < q_c$. Nevertheless, if $q > q_c$, the LD phase appears in segment II. Furthermore, different from model A, the flux J_2 is continuous when crossing the phase boundary $\alpha = \beta$.

The mean field analysis for the critical value q_c and the value of λ at a given q in model B are not so easy to be obtained because there are two types of particles involved. This needs to be further investigated in the future.

5. Conclusions

In this paper, we have presented two different models to investigate the interplay of a totally asymmetric simple exclusion process with a shortcut in its bulk under open boundaries. The phase diagrams of both models can be classified into three regions. However, there are many differences between them: (i) the three regions in model A correspond to the LLL, HHH and MHM phases respectively, while in model B, they are the LLL, HLH or HHH, MLM phases respectively; (ii) the phase boundaries in model A are independent of the value of q, while in model B, they depend on the value of q; (iii) in model A, the phase transition between the LLL and MHM phases are of first order, the phase transition between the HHH and MHM phases is of second order and the bulk densities of all the three segments are linear at the phase boundary $\alpha = \beta$. Moreover, the flux of segment II is discontinuous when crossing the boundary. However, in model B, all the phase transitions are of first order. In addition, at the phase boundary $\alpha = \beta < \lambda$, the bulk densities of segments I and III are linearly independent of q and the bulk density of segment II is linear when $q < q_c$ and is in the LD phase when $q > q_c$. Furthermore, we have obtained the analytical results of model A by using a simple mean-field approximation. It is found the results of the approximate solutions and Monte Carlo simulations are in good agreement.

In our future work, an analytical investigation on model B is needed. Also, the effect of multi-shortcuts will be investigated.

Acknowledgments

We thank Dr W X Wang and Mr J Ren for useful discussion. This work is supported by National Basic Research Program of China (No. 2006CB705500), the NNSFC under Project No. 10532060, 10404025, 70601026, 10672160, the CAS President Foundation, and the Chinese Postdoc Research Foundation (No. 20060390179). R Wang acknowledges the support of the ASIA:NZ Foundation Higher Education Exchange Program (2005), Massey University Research Fund (2005), and Massey University International Visitor Research Fund (2007).

References

[1] Derrida B 1998 *Phys. Rep.* **301** 65
[2] Schütz G M 2000 *Phase Transitions and Critical Pheonomena* vol 19 ed C Domb and J L Lebowitz (London: Academic)
[3] Macdonald J T, Gibbs J H and Pipkin A C 1968 *Biopolymer* **6** 1
[4] Meakin P, Ramanlal P, Sander L M and Ball R C 1986 *Phys. Rev.* A **34** 5091
[5] Kim J M and Kosterlitz J M 1989 *Phys. Rev. Lett.* **62** 2289

[6] Nagel K and Schreckenberg M 1992 *J. Physique I* **2** 2221
[7] Liggett T 1993 *Interacting Particle Systems: Contact, Voter and Exclusion Processes* (Berlin: Springer)
[8] Schadschneider A 1999 *Eur. Phys. J.* B **10** 573
[9] Derrida B, Evans M R, Hakim V and Pasquier V 1993 *J. Phys. A: Math. Gen.* **26** 1493
[10] Schütz G M and Domany E 1993 *J. Stat. Phys.* **72** 277
[11] Evans M R, Rajewsky N and Speer E R 1999 *J. Stat. Phys.* **95** 45
[12] de Gier J and Nienhuis B 1999 *Phys. Rev.* E **59** 4899
[13] Rajewsky N, Santen L, Schadschneider A and Schreckenberg M 1998 *J. Stat. Phys.* **92** 151
[14] Shaw L B, Zia R K P and Lee K H 2003 *Phys. Rev.* E **68** 021910
[15] Lakatos G and Chou T 2003 *J. Phys. A: Math. Gen.* **36** 2027
[16] Mallick K 1996 *J. Phys. A: Math. Gen.* **9** 5375
[17] Evans M R 1997 *J. Phys. A: Math. Gen.* **30** 5669
[18] Chou T and Lakatos G 2004 *Phys. Rev. Lett.* **93** 198101
[19] Kolomeisky A B 1998 *J. Phys. A: Math. Gen.* **31** 1153
[20] Tripathy G 1997 M.Barma *Phys. Rev. Lett.* **78** 3039
[21] Lakatos G, Chou T and Kolomeisky A 2005 *Phys. Rev.* E **71** 011103
[22] Parmeggiani A, Franosch T and Frey E 2003 *Phys. Rev. Lett.* **90** 086601
[23] Popkov V and Peschel I 2001 *Phys. Rev.* E **64** 026126
[24] Popkov V and Schütz G M 2003 *J. Stat. Phys.* **112** 523
[25] Popkov V 2004 *J. Phys. A: Math. Gen.* **37** 1545
[26] Pronina E and Kolomeisky A B 2004 *J. Phys. A: Math. Gen.* **37** 9907
[27] Harris R J and Stinchcombe R B 2005 *Physica* A **354** 582
[28] Mitsudo T and Hayakawa H 2005 *J. Phys. A: Math. Gen.* **38** 3087
[29] Szavits-Nossan J and Uzelac K 2006 *Phys. Rev.* E **74** 051104
[30] Brankov J, Pesheva N and Bunzarova N 2004 *Phys. Rev.* E **69** 066128
[31] Pronina E and Kolomeisky A B 2005 *J. Stat. Mech.* P07010